

# ISRG Journal of Engineering and Technology (ISRGJET)



ISRG PUBLISHERS

Abbreviated Key Title: ISRG J Eng Technol.

ISSN: 3107-5894 (Online)

Journal homepage: <https://isrgpublishers.com/isrgjet/>

Volume – II Issue – III (May-June) 2026

Frequency: Bimonthly



## Prediction of Bearing Capacity of Thermally Treated Soft Clay Using Artificial Intelligence and Heated Borehole Method

Ali H. Shareef<sup>1\*</sup>, Mohammed A. Al-Neami<sup>2</sup>, Abdulelah A. AlHumrani<sup>3</sup>, Falah H. Rahil<sup>2</sup> & Hayder A. Al-Sudani<sup>4</sup>

<sup>1</sup>Lecturer, Building school Department, Ministry of Education / Rasafa 3– Iraq.

<sup>2</sup>Professor, Civil Engineering Department, University of Technology – Iraq.

<sup>3</sup>Assistant Lecturer, Building school Department, Ministry of Education / Rasafa 3– Iraq.

<sup>4</sup>Assistant Lecturer, Prime minister's office, Baghdad– Iraq.

| Received: 07.05.2026 | Accepted: 14.05.2026 | Published: 27.05.2026

\*Corresponding author: Ali H. Shareef

### Abstract

Soft clay soils are known as problematic geomaterials due to their low bearing capacity, high compressibility, and large amounts of settlement, which greatly affect the stability and performance of civil engineering structures. This research explores an experimental and data-driven framework for investigating the strength of soft clay using the heated borehole method to improve soft clay's bearing capacity by using artificial intelligence (AI) based modeling. To create thermal treatment within the soil mass, a field-simulated heating system was developed using locally available cooking gas. The effects of borehole spacing, borehole depth, borehole heating duration, and bores' pattern were systematically examined using laboratory model footing tests. The results show that thermal treatment improved the strength of the soil and the bearing capacity of the soil. The optimal conditions were found to be 3D spacing, 2b depth, and approximately 8 hours for heating duration. Compared to arrangements in a circular or triangular shape, the arrangement that is square produced the maximum improvement. Furthermore, predictive models such as GLMs, SVR, and polynomial were used in relation to the experimental dataset. Of these three predictive models, polynomial had the best results with a coefficient of determination greater than 0.98. Therefore, the predictive equations developed are a reliable method for estimating the bearing capacity of thermally treated soft clay, providing geotechnical engineers with a useful and efficient method of accomplishing their work.

**Keyword:** Borehole, Bearing capacity ratio ( $q_u/C_u$ ), Thermal, Artificial intelligence (AI), Spacing, Pattern, improvement.

## 1. Introduction

Weak soil types, such as clay soils, can cause issues when building close to or on them. Soft clay is amongst the most problematic types of soil for construction projects that are carried out in low-energy areas, such as lowland or coastal zones (where industrial and urban centers are usually developing) [1]. As such, soft clay is found to have high plasticity, be dispersible, have high compressibility, have the potential to swell, be very weak in shear and easily influenced by environmental effects, all of which causes poor performance from a construction perspective and ultimately leads to significant amounts of deformation under the actions of loading [2]. Regardless of the type of soft clay, its construction performance needs to be improved so that we can build safely and continue to do so in the future. The three main categories of ground improvement techniques are chemical, biological and mechanical stabilization [3, 4]. More recently, an alternative technique which modifies engineering behavior of weak soils is via thermal treatment. This includes baseline studies on the effect of elevated soil temperature on various aspects of soil properties and have shown significant improved performance of soils [6, 5]. For instance, existing literature illustrates an increase in temperature will greatly affect (i.e., increase or decrease) the specific gravity, maximum dry density and optimum moisture content of clay soils over a broad range of temperatures [7]. Additionally, previous studies have demonstrated that heating decreases the plasticity index, swelling pressure and moisture content with the exception of when soil conditions yield decreased undrained shear strength (depending on multiple variables) [8]. As the temperature increases, clay soils experience a number of complex physicochemical transformations, including changes in mineralogy, thermally induced microcracks, and restructuring of soil particles [9]. These transformations have a very important effect on the soil's thermophysical properties which are related to thermal conductivity, where thermal conductivity has been found to correlate strongly with soil density [10]. Higher warming practices through advanced methods such as microwave treatment have been shown to enhance soil stability while also limiting swelling behaviour, but they can also increase internal porosity and cracking within the soil [11–12]. Additionally, the length of time heating an area has a major impact on how soils will respond to heat, and in most cases the relationship will be nonlinear between heating time and the soil's density, saturation level, and volume changes [13–14]. Numerous studies have proposed mathematical equations relating to the temperature-dependent variation in parameters of shear strength (cohesion, internal friction angle). Some studies have examined how temperature affects the dielectric properties of expansive soil and the effectiveness of microwave heating at altering expansive soils, demonstrating a correlation between heating time and a decrease in swelling characteristics. Therefore, since temperature and time are the main variables affecting the behavior of soils treated with thermal energy, further investigation of these two variables will lead to an improved understanding of how thermally treated soils behave. While technological advances have been made, most available research employs laboratory heating systems that do not closely replicate actual field situations (e.g., conventional furnaces or controlled microwave settings). In addition, thermally treated soils exhibit complicated behavior as a result of numerous interrelated variables: distance, depth, temperature, heating time, and geometric arrangement. Also, these variables relate to one another in a highly nonlinear manner. Because of these complexities,

traditional analytical methods will not work well to predict soil behavior. To overcome these limitations, the research combines experimental research with data-driven methodologies and modeling methodology for artificial intelligence. Specifically, the research relied on current AI techniques, including statistical analysis using ChatGPT, and regression techniques using machine-learning to analyse the experimental data set and determine the relationships between soil bearing capacity and the associated key variables. This allowed for the efficient handling of complex non-linear interactions and the development of equations that provided a reliable and accurate prediction. The goal of this research was to create a new system to thermally treat soil by using heated boreholes. Locally available cooking gas was the heat source for this system, which allowed the system to be practical and feasible for implementation in local areas, such as Iraq, due to abundant energy resources. The investigation evaluated the impact of borehole spacing, borehole depth, duration that the boreholes would be heated, and the geometric shape of the boreholes on the improvement of soft clay soil behavior when subjected to a load. In addition, the experimental data from this study was analyzed using a combination of statistical and artificial intelligence analysis techniques, including generalized linear models, regularized regression methods, support vector regression, and polynomial regression. A new method was developed that combines ChatGPT assistive analytical support with several modeling techniques to easily identify the best predictive modeling method and create mathematically accurate relationships from which predictions regarding the bearing capacity of soil could be made. This study was completed in order to assess the effectiveness of thermal treatment, using heat wells, on improving the mechanical properties of soft clay and to produce accurate predictive modeling equations for estimating the bearing capacity of soil based on numerous variables. The uniqueness of this study is combining a field-simulated heat system with artificial intelligence (AI) analytical techniques in order to provide practical and accurate predictive tools for use in geotechnical engineering.

## 2. Methodology and Experimental Work

### 2.1. Material Used

In the experiment, three main types of materials were used: soil, gas and water. The soil sample used for this project was taken from the Al-Amer district of Baghdad City; the physical and chemical properties of the soil at that location are provided in Table (1) and a graphical representation of soil particle size distribution is provided in Figure (1). The heat source used for this experiment was liquefied petroleum gas (LPG), which is a pressed gas kept under high pressure in gas cylinders. It consists mainly of methane along with propane, ethane and some heavier hydrocarbons. It also contains small amounts of nitrogen, hydrogen sulfide, carbon dioxide and water. LPG will typically burn efficiently when it is mixed with air in a volumetric ratio of four to twelve percent [18]. Lastly, tap water was used throughout the experiment for preparing and conditioning the soil.

**Table (1):** physic-chemical properties of soil.

Index Property	Index Value
Liquid Limit (%)	45
Plastic Limit (%)	23
Plasticity Index (%)	22

Specific Gravity	2.69
Gravel %	0
Sand %	2
Silt %	20
Clay %	78
Classification (USCS)	CL
Organic Matter (%)	< 0.01
Total Dissolved Salt (%)	2.21
Total Solved Salt (%)	8.3
pH Value	7.2

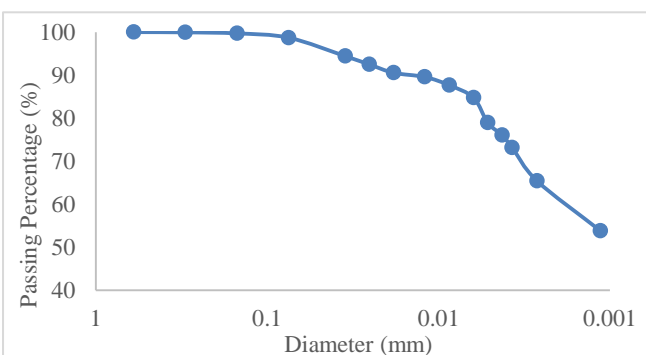


Figure 1: Grain size of soil.

## 2.2. The devices and Tests Used in This study

To analyze how soft clay behaves when subjected to thermal conditioning, simulating the field as closely as possible was imperative. A specific design and fabrication were applied to develop the test apparatus and components for the research purpose. The system would be capable to create controlled heating in the soil mass with a following application of a static load applied to a model footing (200 mm x 200 mm). The experimental system was composed of four principal components: metal load framework; soil container (metal box); borehole casing (barrier tube); heating system.

### 2.2.1. Metal Load Framework

A loading frame constructed of steel to create a vertical alignment of the piston to apply a central concentrated load to the treated soil was designed. The load was applied through the soil model within a metal container (dimensions of the container 92.5 x 92.5 x 92.5 cm<sup>3</sup>) and transferred via the loading frame. The framework was also used to support a motor for the installation of borehole casing during the preparation and heating phases. The loading system configuration is illustrated in Plate (1).

### 2.2.2. Casing (Barrier Tube)

Well casing was constructed from carbon steel pipe that meets the material standards set forth in ASTM A53 Grade B. Each casing is 43 mm in outside diameter, with a wall thickness of 4 mm. The physical characteristics of the casings are summarized in Table (2). Each casing was installed at different lengths, which correspond to the location of 1b, 1.5b, 2b, and 2.5b from the face of the model footing, with b representing the footing's width (for the purposes of determining length). Plate (2) shows the different casing configurations. Tested results show a minimum borehole diameter of approximately 35 mm is required to allow for combustion in the

surrounding soil. Thus, when developing an effective heat source and delivering heat into the surrounding soil, sufficient space must be provided for heat generation and transfer [19].

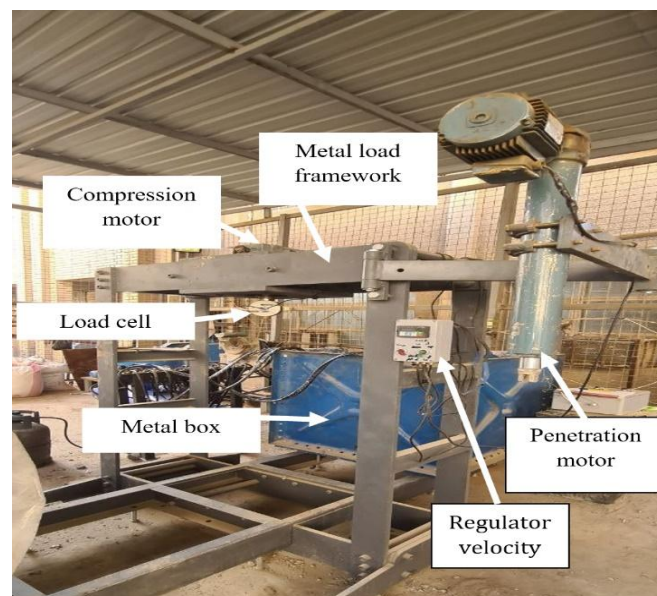


Plate (1): Metal load framework



Plate (2): Case tube of the borehole

Table (2): The physical properties of pipe cases

Properties	Values
Density at 20 °C (Kg/dm <sup>3</sup> )	785
Thermal conductivity at 20 °C (W/m.K)	50
Specific thermal capacity at 20 °C (J/Kg.K)	460

### 2.2.3. The System of Heating

The constructed heating system was designed and installed with the purpose of generating a controlled thermal energy source within the soil model, as would be found in a field application. The heating system consisted of five key components. The first component was the combustion pipes which initiated and maintained heating within the borehole casing. The second component was the high-pressure rubber piping (W/BP 20/30 BAR) which transported the gas-air mixture from the source to the combustion pipes. The third component was a control unit, which received the signal from the gas cylinder, in order to control the heating source, and maintain a stable combustion and heating process during the entire testing period. The fourth component was an air compressor, which supplied the necessary air flow for combustion. Lastly, there was the use of a gas cylinder and a gas regulator to control the fuel supply. The overall configuration of the heating system can be seen in Plate 3. Two different measurement systems, one internal and one external, were used for

providing reliable and accurate temperature monitoring. While using one external unit (the control panel) with the other internal unit (the thermal sensors), the two temperature controllers connected through thermal sensors were used to measure the in-situ temperature of the soil during heating. The control panel has 2 switches for turning on/off each of the 2 temperature controllers; as well, the control panel has lamps to show whether the entire system is operating. The second temperature recording system contained five separate thermocouples inside of the soil body. All of these thermocouples were connected together using a thermal cable. Each thermocouple is 30 cm long and is aligned in such a way as to measure temperature at various depths in the soil during the period of time that the soil was being heated. The thermocouples have been connected to a data logger (Ordell 100) to record the temperature readings on a continuous basis and retain those temperature readings for future analysis in a digitized form. In order to improve accuracy and repeatability of the experimental results, two different models have been created for every type of test. One model is equipped with seven thermal sensors which will show a detailed temperature distribution, while the other model has been equipped with two thermal sensors for the purpose of validating the data from the first model. This dual configuration will help to confirm the reliability of the temperature data collected as well as reduce uncertainty in measuring.

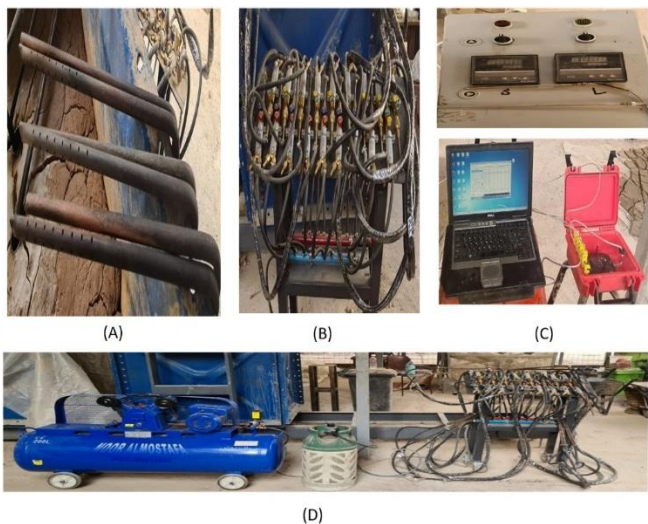


**Plate (3):** The System of Heating ((A) combustion pipes, (B) the control of the heating source, (C) measuring devices of the heating system, and (D) air compressor, the gas bottle, and gas regulator)

### 2.3. Establishing The Soil Modelling and Test Procedure

The undrained shear strength of the soil was determined to be 14 kPa through the mixing of dewatered clay soils with the addition of 29% moisture content to the final product, which was achieved by mixing 25 kg of dry clay soil with 29% water for an approximately equivalent weight of 40 kg of wet clay soil. In addition to this test was performed using a portable vane shear device to measure the undrained shear strength of the freshly prepared clay soil. Due to the laboratory mixing process of clay and water yielding an inhomogeneous material, the final product will be mixed utilizing the 120 L laboratory scale mixer to create a homogeneous output. After completion of mixing, the clay soil will be transferred into polythene bags and stored for a period of 24 hours to allow for moisture distribution throughout the sample. The final stage includes loading the final product into the test cube which has interior dimensions of 92.5 cm × 92.5 cm × 92.5 cm; the clay will

be placed in 10 cm layers and compacted with a 6 cm × 6 cm wooden tamper during compaction until reaching the point of completion for the test sample (i.e., the top surface will be cleaned and levelled prior to initiating the max/min testing). An inflexible wooden board with equivalent ground level dimensions was put on the ground and increased 5 kPa of pressure to settle for a period of 24 hours to settle, consolidate, and provide consistent ground level data. After the settlement of the wood plate, a guide plate was placed to organize the design and distribution of the bore holes per the needed distribution and distance between them. After that nine bore hole casings were placed in the ground using a hydraulic percussion process, and bore hole casing soil was removed by drilling using an auger measuring 34.5 mm in diameter. After the augering of the bore hole casings was complete the guide plate and the hydraulic penetration unit were removed and prepared the earth model for heating. To start the heating process, combustion tubes were placed into the bore hole casings. A combination of air and a gas in the form of an air/gas mixture that contains 10% gas and 90% air has been provided to the system; ignition was induced by means of pipe primers. After the establishment of the combustion process heat from the casing is lost to the surrounding soil, beginning the thermal treatment process. After the heating phase has been completed, the system was turned off, and the soil model was left to cool slowly to ambient temperature for a period of 24 hours before being resampled.

After cooling, the model footing (20 cm x 20 cm) was placed at the center of the soil surface. Proper alignment of the loading system was established in order to position the footings correctly and a monotonic vertical load was applied with a motorized loading device at a constant rate of 1 mm/min. Load and settlement were measured using load transducer and Linear Variable Differential Transformer (LVDT). Whereas the traditional method for defining failure in shallow foundation tests is when the settlement reaches 10% of the width of the footing, this method was found to be inadequate in this study. Surface cracks developed as a result of water vapor escaping through the heating process caused the traditional definition of failure to be inadequate. Thus, failure was established at a settlement equal to 15% of the footing width or greater. This provides a more significant value for the ultimate equilibrium loading capacity in the tested environment. The full sequence of soil preparation, heating, and load testing is shown in Plate (4).



**Plate (4):** Stages of test procedure of soil improvement by heating for load test

### 2.4. The Testing Program in This Research

The research approach used in this study is constrained to a series of four sequential processes including the analysis of physical models, as shown in the figure (2).

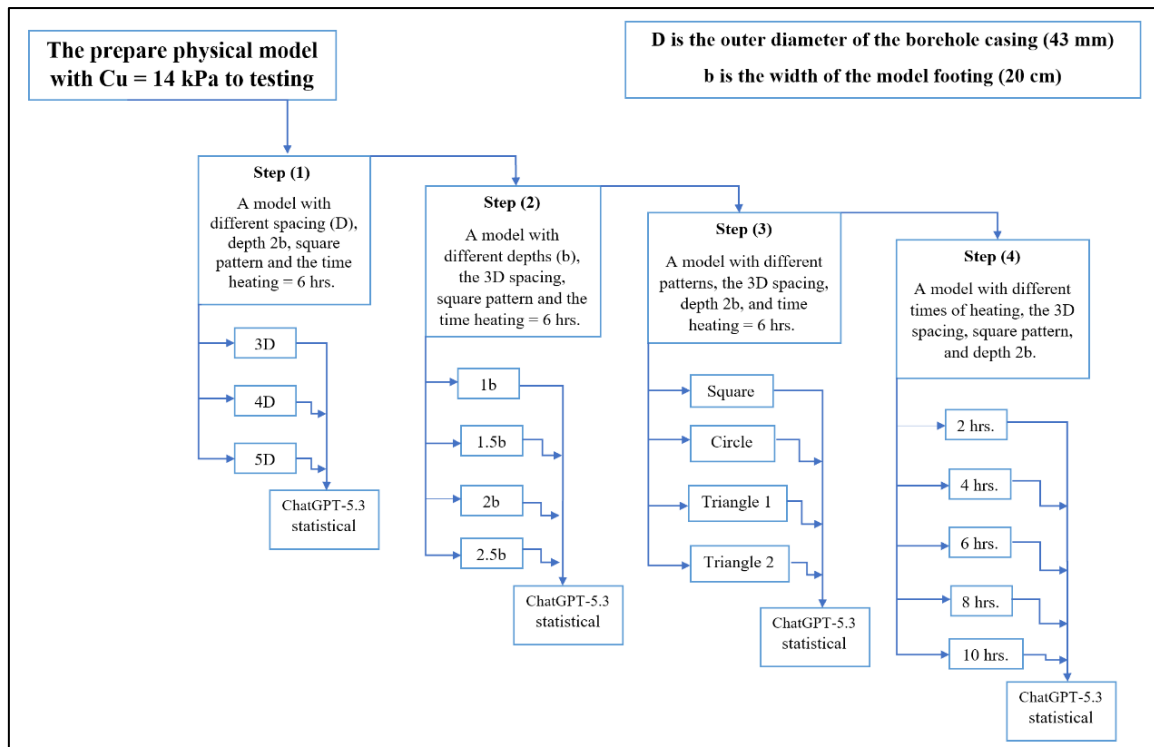


Figure 2: Schematic representation of the experimental workflow for the testing program.

### 3. Presentation and Discussion of Test Results

#### 3.1. The Impact of Distance Between Boreholes Casing (Spacing)

The investigation used 9 boreholes arranged in a square pattern, with a diameter of 3.5 cm and a length of 40 cm (2b in length). The boreholes were spaced 3D, 4D, and 5D apart and were excluded from 2D due to inefficient burning and to minimize CO<sub>2</sub> emissions. The total heating time was 6 hr, as per Rahil [19]. The results showed an improvement in the bearing ratio of the thermally-treated soil compared to the untreated soil. The best improvement occurred at 3D spacing; however, the improvement diminished at 4D and 5D as shown in Figure (3). Additionally, the mode of failure for untreated soils was punching failure, while for treated soil, it was general shear failure, which reflected that treated soil has a significant improvement in soil behaviour due to thermal treatment. The temperature-time response measured at the midpoints of boreholes, at thermo-cable depths of 0.15 m (15 cm) and 0.30 m (30 cm), is illustrated in Figures (4) and (5). As you can see, the highest temperatures were measured with a 3D borehole-to-borehole spacing, where the temperature decreased with increasing spacing. The reason for this finding is the thermal interaction between the boreholes; that is, the closer the borehole-to-borehole spacing, the greater the overlap of the heat-affected zones, thus allowing for much more effective heat transfer from adjacent boreholes, as shown in Plates (5) and (6). The thermal treatment improved the physical performance of the soil, by reducing the moisture content of the soil and changing the physicochemical properties of the soil. This, in turn, resulted in increased shear strength and bearing capacity of the soil. To quantify the total effects of settlement ratio, borehole spacing, and temperature, the experimental data were analyzed using advanced AI statistical modelling techniques. Of the techniques analyzed, Polynomial Regression had the best performance based on a

coefficient of determination of 0.991, which indicates a strong correlation between predicted and experimental values. Accordingly, the following predictive relationship was developed:

$$\left(\frac{q_u}{C_u}\right) = 22.08 - 482.99 \left(\frac{\text{Settl.}}{b_{\text{footing}}}\right) - (10^{-6})D - (35 \times 10^{-7})T - 118.973 \left(\frac{\text{Settl.}}{b_{\text{footing}}}\right)^2 + 6.41 \left(\frac{\text{Settl.}}{b_{\text{footing}}}\right)D + 1.233 \left(\frac{\text{Settl.}}{b_{\text{footing}}}\right)T - (22 \times 10^{-6}) - (123 \times 10^{-5})DT - (6 \times 10^{-5})T^2 \quad (4.1)$$

Or

$$q_u = (22.08 - 482.99 \left(\frac{\text{Settl.}}{b_{\text{footing}}}\right) - (10^{-6})D - (35 \times 10^{-7})T - 118.973 \left(\frac{\text{Settl.}}{b_{\text{footing}}}\right)^2 + 6.41 \left(\frac{\text{Settl.}}{b_{\text{footing}}}\right)D + 1.233 \left(\frac{\text{Settl.}}{b_{\text{footing}}}\right)T - (22 \times 10^{-6}) - (123 \times 10^{-5})DT - (6 \times 10^{-5})T^2)C_u \quad (4.2)$$

Where:

$q_u$ : Compressive stress for treated soil (kPa)

$C_u$ : undrained shear strength of untreated soil (kPa)

Settl.: settlement (mm)

$b_{\text{footing}}$ : Width of footing test

D: Spacing between boreholes casing (cm)

T: Degree of temperature (°C)

One of the major results of this study is the equation because it combines mechanical and thermal effects into a single prediction framework. The high value of demonstrates that the currently used AI-Based Model (based on ChatGPT-5.3) can well represent the interaction of settlement, spacing and temperatures. As such, this equation represents a valuable, precise tool to determine the bearing capacity of thermally treated soft clay material based on the data of this particular research. The developed model is

applicable to square borehole patterns, a borehole depth of 6.0 m, offset spacing of 2.25 m or more, heating duration of 6 hours and

temperature readings at the model's central point.

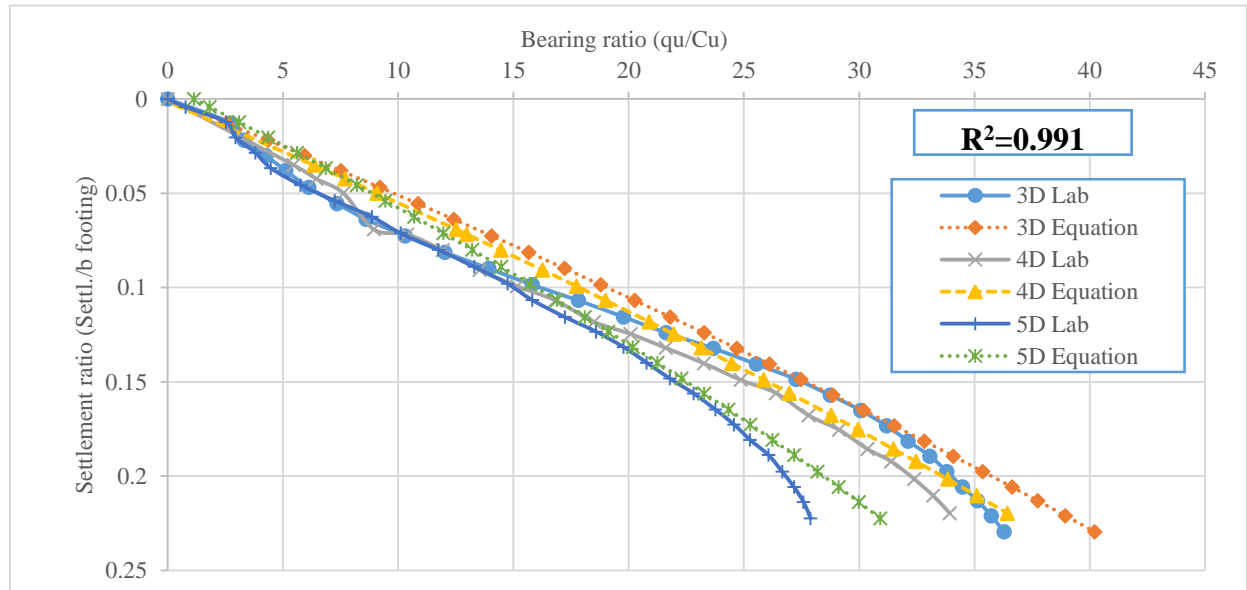


**Figure (3):** The connection dimensionless between the bearing ratio lab, the bearing ratio proposed equation (4.1) and the settlement ratio for various spacing models

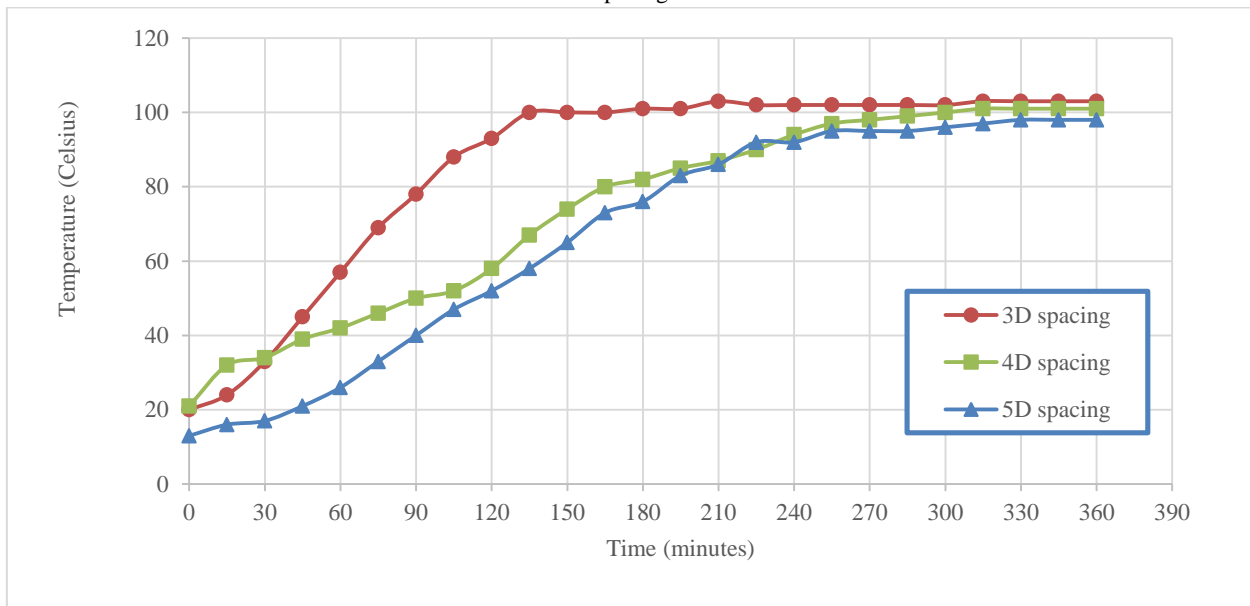


**Figure (4):** The relationship between the temperature and the duration time for the 15 cm length of thermos-cabal with various spacing

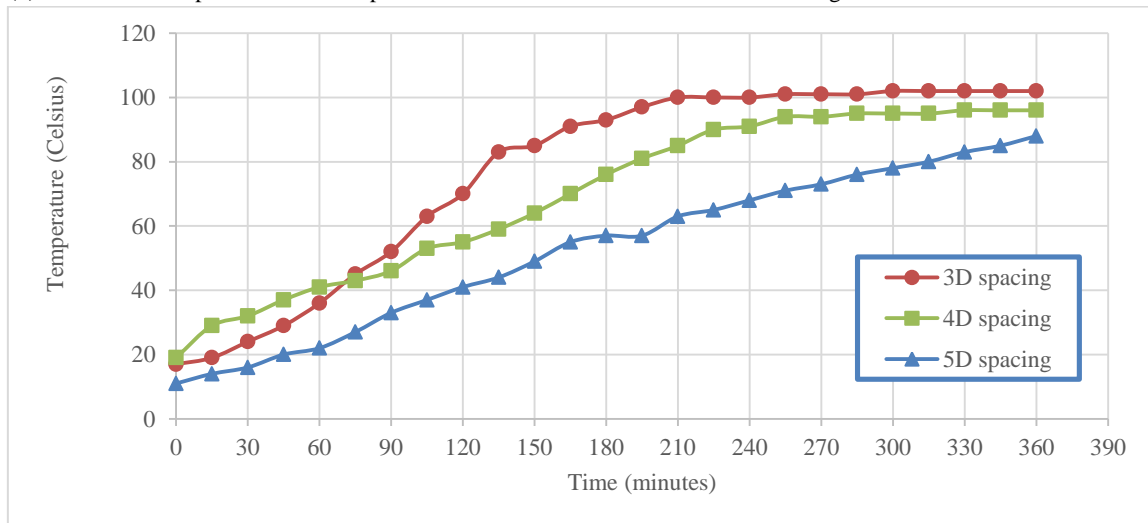


**Figure (5):** The relationship between the temperature and the duration time for the 30 cm length of thermos-cabal with various spacing



**Plate (5):** The enhancement area by the heating technique of the 3D model



**Plate (6):** The enhancement area by the heating technique of the 5D model

### 3.2. The Impact of Boreholes Casing Depth

Results from the experiments clearly show that an increase in the depth of borehole casing substantially improves the bearing capacity of thermally treated soft clay. However, this does not follow a linear pattern: when the depth reaches an optimum but is greater than 2.5, there is little to no increase in the bearing ratio with an increase in depth (see Figure 6). For example, the bearing ratio increases from 14.2 at 1 to 28.2 at 2.5; hence the relationship is not linear. This behavior indicates the fundamental relationship between the thermally treated zone and the stress distribution beneath footings. The area affected by thermal effects is at a temperature range below and below below. At this shallower depth (i.e., at depths =70 meters (230 ft)), the treated area of the borehole does not overlap with maximum stress area. Thus, limited increase in bearing capacity to treated soil. At greater depths (e.g., when the borehole reaches a depth of greater than 70 meters), the treated area is fully (overlapping) with the maximum stress area, producing increased soil stiffness and shear strength. This fully

defined configuration provides the most efficient thermal treatment by creating a thermal improvement within the soil volume directly responsible for transferring the loads from primarily vertical loads and/or from lateral loading. The addition of depth into the response curves results in only small increases in performance. The reason for this is due to the dissipation of stress with depth. When a load is applied, much of the load has already been transmitted to an upper layer, which means that any thermal treatment provided beyond this effective stress zone will have little effect on the overall bearing capacity resulting in diminishing returns. This finding corresponds well to the classical stress-bulb theory, which states that the performance of thermal improvements is dependent on the level of stress exerted on a particular area rather than on its absolute depth. The experimental data were analyzed with respect to quantifying this complex nonlinear behaviour by employing an advanced statistical method based on artificial intelligence (AI) (Localised refusal message). The constructed polynomial model is among the most important deliverables of this research, demonstrating that the polynomial model accurately represents the interrelationship between settlement and borehole depth. This predictive relationship is shown below:

$$\left(\frac{q_u}{C_u}\right) = (364.23 - 22.78d + 0.3779d^2) \left(\frac{\text{Settl.}}{b_{\text{footing}}}\right) + (-4662.59 + 375.61d - 5.4898d^2) \left(\frac{\text{Settl.}}{b_{\text{footing}}}\right)^2 + (11633.73 - 1012.77d + 14.9309d^2) \left(\frac{\text{Settl.}}{b_{\text{footing}}}\right)^3 \quad (4.3)$$

**Where:**

$q_u$ : Compressive stress for treated soil (kPa)

$C_u$ : undrained shear strength of untreated soil (kPa)

Settl.: settlement (mm)

$b_{\text{footing}}$ : Width of footing test

$d$ : depth of boreholes casing (cm)

This equation is significant because it integrates the governing parameters into one single predictive framework that reflects the true nonlinear behaviour of thermally treated soil. Furthermore, the coefficient of determination is high enough to demonstrate that the AI-based (ChatGPT-5.3) ( $R^2 = 0.994$ ) model is powerful and dependable in replicating the experimental behaviour. Compared with traditional empirical relationships, this model contains higher-order interaction terms, resulting in an improved ability to depict the total effects of deformation and depth on one another. The developed model is valid under the following conditions: square arrangement of boreholes was used; borehole depths were between; heating time was six hours; and the temperature measuring point was at the centre of the model.

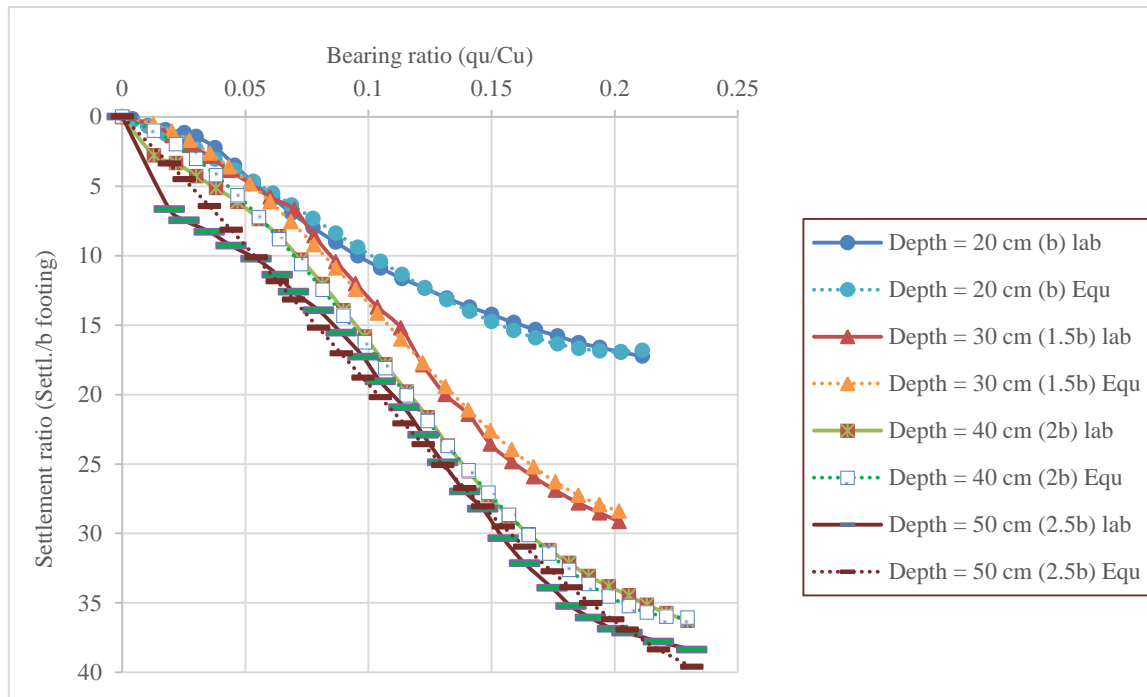


**Figure (6):** The connection dimensionless between the bearing ratio lab, the bearing ratio proposed equation (4.3) and the settlement ratio for various depth models

### 3.3. The Impact of Borehole Casing Pattern

The results show that the Pattern of boreholes, compared to both spacing and heating depth, has a secondary effect on the bearing capacity of the boreholes, but even so, it produces a significant difference in the overall temperature distribution between the Square, Circle, Triangle 1 and Triangle 2 patterns. The Circle generally recorded the highest temperatures compared to the other two patterns, which experienced relatively low thermal responses respectively. However, the differences in the borehole arrangement did not produce a corresponding amount of change in the Bearing Capacity Ratio due to the different shapes of the borehole arrangements, as illustrated in Figure 7, so temperature itself is not the only driving factor. Figures 8 and 9 provide plots of the Time Dependent Temperature Variations at the mid-points of the treated zones across all of the test shapes for both 15 cm and 30 cm lengths of Thermocable.

The treated zone's modularity and spatial coherence below the footing mainly regulate the improvement process rather than its peak temperature. The square and circular patterns provided a more consistent heat distribution throughout, generating interlocking treated unit cells, which improve the efficiency of load transfer. The triangular pattern created an inconsistent and dispersed treated zone, which diminished the interlocking effect, resulting in lower ultimate bearing capacities. Due to the inconsistent nature of the treated area below the footing in triangle pattern 1 and 2, lower levels than that of the square pattern occurred, as seen in Plate 7. Despite the circular pattern reaching higher peak temperatures, the bearing capacity ratio remained just below that of the square pattern (Plate 8). Therefore, while the maximum temperature influences improvement, the uniformity of treatment is more important than the maximum temperature. In order to quantitatively assess and quantify the magnitude of this behaviour, experimental data were subjected to analysis through an advanced

AI-based predictive model. As a result of this analysis, a predictive equation was developed that displays a strong correlation between bearing capacity ratio and its governing variable(s), thus supporting the theory that the efficiency with which load can be transferred is dictated more by geometric continuity of the treated area than it is by simply the amount of heat administered. This equation represents one of the most important contributions from the study; it turns difficult to interpret experimental data into an easy-to-use predictive tool that can then be used on engineering design & optimization of thermal soil improvement methods.

$$\left(\frac{q_u}{C_u}\right) = S_F((95 + 0.15T + 0.02t)\left(\frac{\text{Settl.}}{b_{\text{footing}}}\right) + (850 + 1.8T + 0.3t)\left(\frac{\text{Settl.}}{b_{\text{footing}}}\right)^2 + (2400 + 3.5T + 0.5t)\left(\frac{\text{Settl.}}{b_{\text{footing}}}\right)^3) \quad (4.4)$$

Where:

$q_u$ : Compressive stress for treated soil (kPa)

$C_u$ : undrained shear strength of untreated soil (kPa)

Settl.: settlement (mm)

$b_{\text{footing}}$ : Width of footing test

$T$ : Degree of temperature ( $^{\circ}\text{C}$ )

$t$ : Duration heating time (minutes)

$S_F$ : = Shape factor (Circle = 0.55, Square = 0.64, Triangle= 0.38-0.41).

The developed equation was established based on the following conditions: the temperature was measured at the center of the model, spacing greater than  $2D$ , the borehole depth was fixed at  $2b$ , and the equation is recommended for spacing greater than  $2D$ .

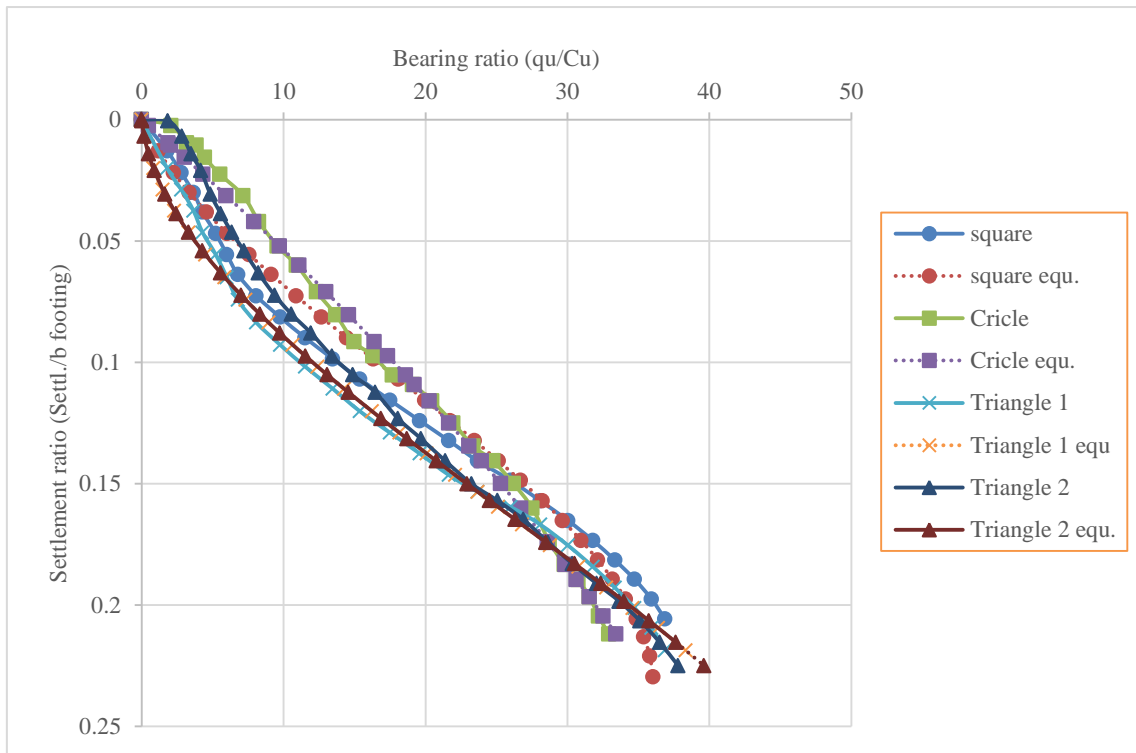


**Figure (7):** The connection dimensionless between the bearing ratio lab, the bearing ratio proposed equation (4.4) and the settlement ratio for various heating duration time models

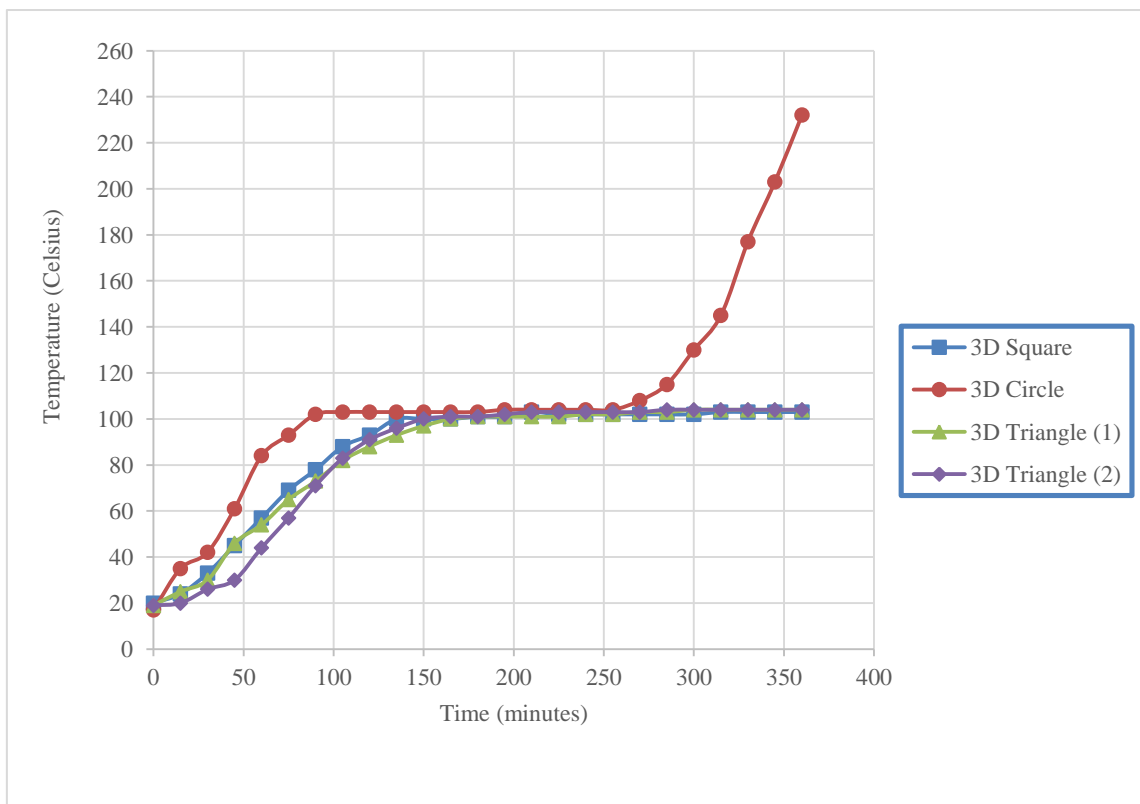


**Figure (8):** The relationship between the temperature and the duration time for the 15 cm length of thermo-cabal with various pattern

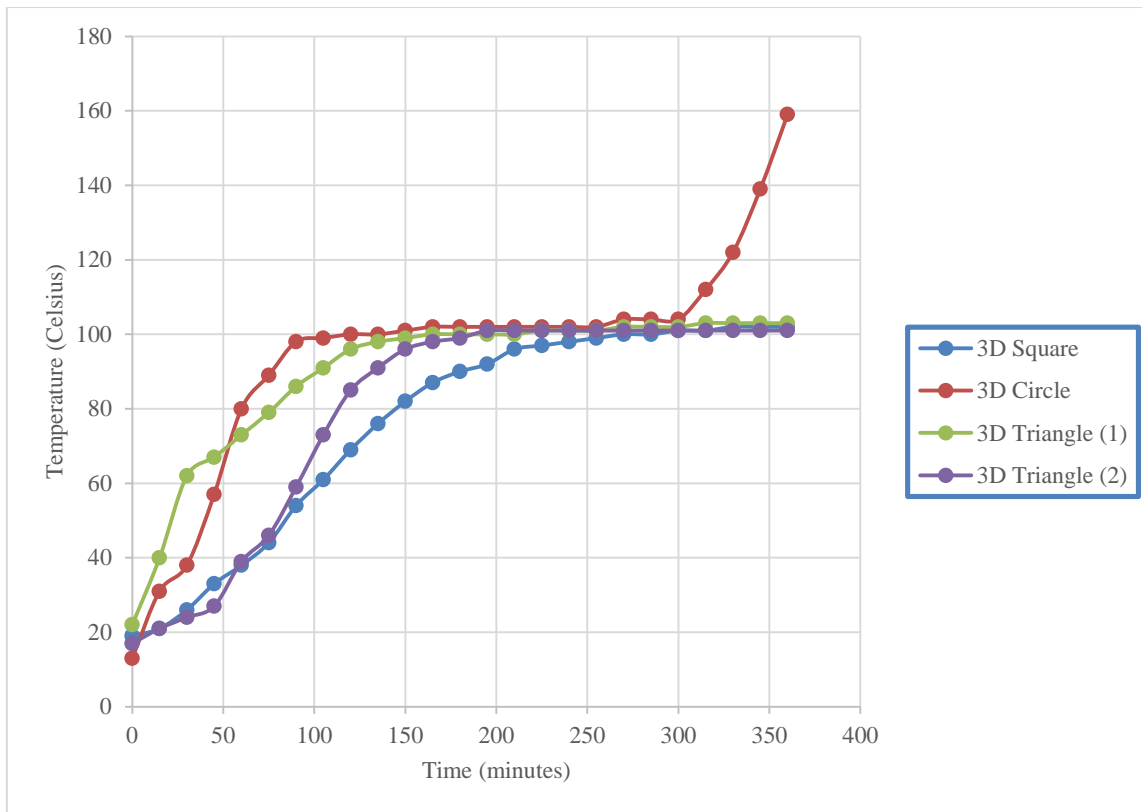


**Figure (9):** The relationship between the temperature and the duration time for the 30 cm length of thermo-cabal with various pattern



(A)

(B)

**Plate (7):** The triangular pattern model ((A) triangle (2) (existence two borehole heating casing under footing), and (B) triangle (1) (existence one borehole heating casing under footing))



**Plate (8):** The circular pattern model

### 3.4. The Impact of Heating Period on Behavior and Strength of Treated Soil

To assess the effect of heating time on bearing capacity, five heating conditions with a 9 square borehole arrangement (boreholes (3.5 cm diameter and 40 cm depth)) were utilized. Heating times were 2, 4, 6, 8 and 10 hours, with the distance of the boreholes from each other and the depth remained constant (3D and 2b). Temperatures recorded at the midpoint of each heating treatment were taken for 15 cm and 30 cm lengths of thermo-cable. The results demonstrated a three-phase heating pattern. The first was a rapid rise in temperature at a rate of approximately 67 °C for the first 120 minutes due to efficient heat transfer from saturated soil. The second was steady-state temperature data recorded between 120 – 360 minutes at an average of 101 °C due to moisture evaporating. The third was a steep rise in temperature after 360 minutes when the saturated soil had dried out and the only way that heat was transferred was through conduction through the soil particles. This indicates that the transition from efficient heat transfer to inefficient heat transfer occurred at approximately six hours of heating. As seen in Figure 12, the duration of heating affects the bearing ratio; however, this effect appears mostly at approximately a 15% settlement ratio. The effect is primarily due to increased shear strength parameters and particularly internal friction angle. It causes soil to behave more like that of a granular material. This phenomenon has been described quantitatively using an AI-based regression model, which produced the following equation:

$$\left(\frac{q_u}{C_u}\right) = -52.93 + 468.7 \left(\frac{\text{Settl.}}{b_{\text{footing}}}\right) + 1.5T - 1.3t - 178 \left(\frac{\text{Settl.}}{b_{\text{footing}}}\right)^2 - 2.25 \left(\frac{\text{Settl.}}{b_{\text{footing}}}\right) T + 141.6 \left(\frac{\text{Settl.}}{b_{\text{footing}}}\right) t - 10^{-3}T - 10^{-2}Tt + 6.03t^2 \quad (4.5)$$

**Where:**

- qu: Compressive stress for treated soil (kPa)
- Cu: undrained shear strength of untreated soil (kPa)
- Settl.: settlement (mm)
- b<sub>footing</sub>: Width of footing test
- T: Degree of temperature (°C)

t: Duration heating time (minutes)

The model exhibits excellent agreement with experimental data ( $R^2 = 0.988$ ), confirming that bearing capacity is governed by the combined effects of settlement ratio, temperature, and heating duration rather than by a single parameter. The proposed equation is valid under the following conditions: square borehole pattern, borehole depth of 2b, spacing greater than 2D, and temperature measured at the center of the model.

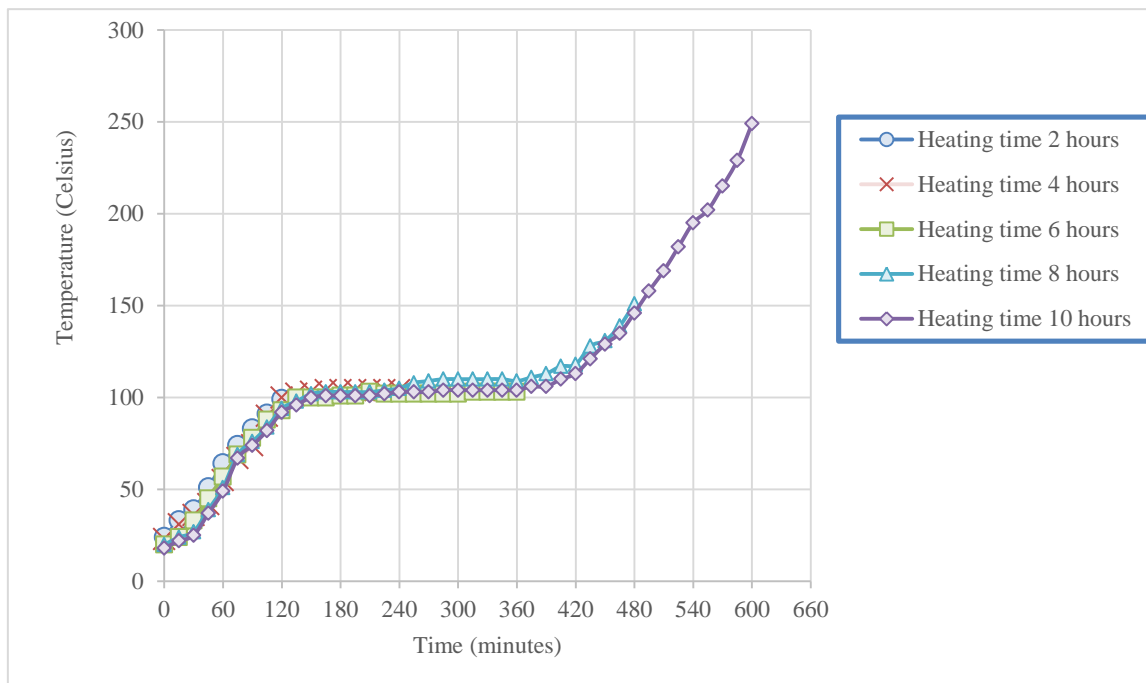


**Figure (10):** The relationship between the temperature and the duration time for the 15 cm length of thermo-cabal with various duration heating time

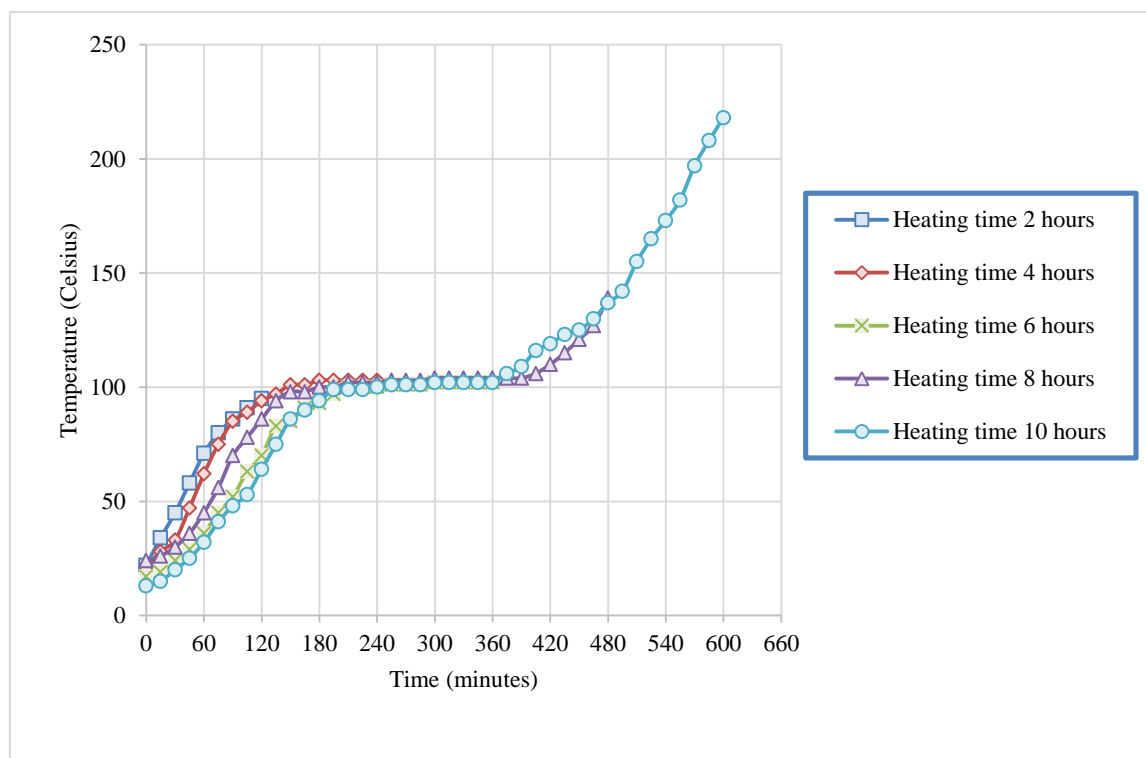


**Figure (11):** The relationship between the temperature and the duration time for the 30 cm length of thermo-cabal with various duration heating time

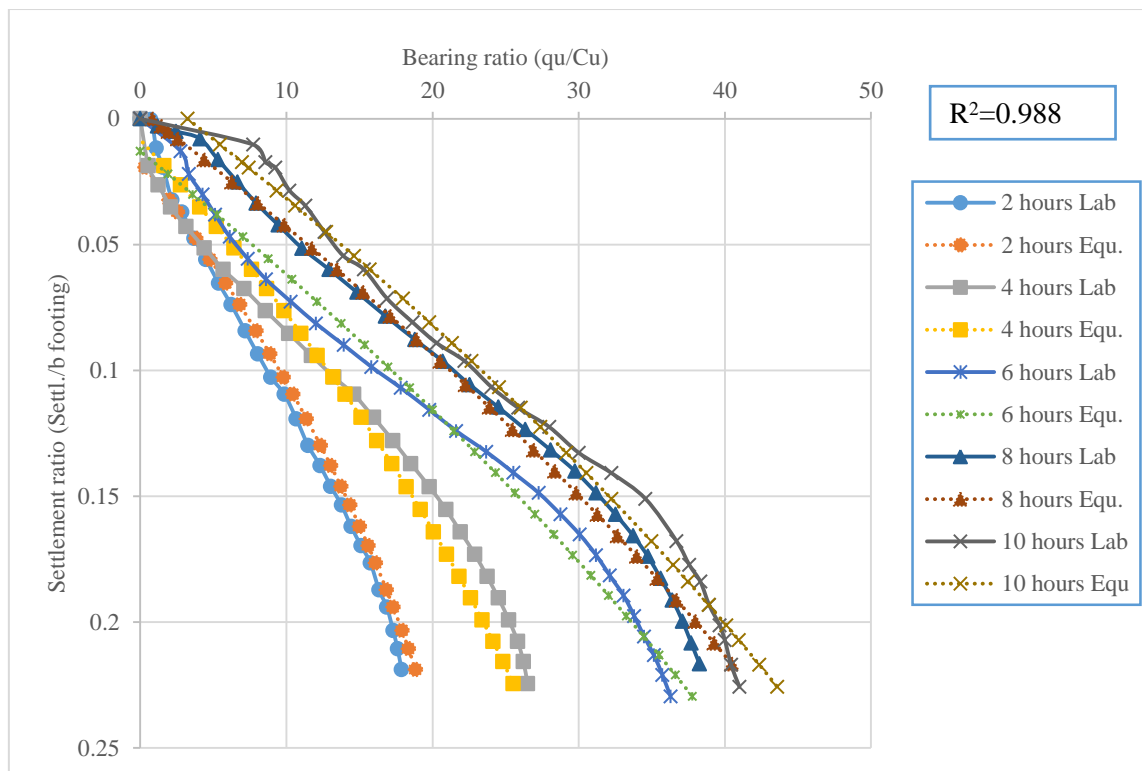


**Figure (12):** The connection dimensionless between the bearing ratio lab, the bearing ratio proposed equation (4.5) and the settlement ratio for various heating duration time models

#### 4. Conclusion

- The performance of the Rafael Brammer (Brammer) Borehole heating system has shown that it reduces soft clay's load-supporting ability but does reduce how much that clay settles under load.
- Borehole depth and spacing are the most significant parameters on the performance of the Brammer system. The best configuration had boreholes at a spacing of  $3D$ , and depth of  $2b$ , where the average treated zone will overlap the stress bulb.
- The way the hole is bored may also affect the performance because even though a circular borehole produced better temperatures than the square was achieved more consistently with continuous treatment.
- The length of time the soil is heated affects how it behaves. It was observed that three different phases of the heat-treated soil existed, with a noticeable change occurring at about 6 hours.
- Almost all of the bearing capacity increase for heated soil occurred in the first 6 hours, with a decrease after that in how quickly the bearing capacity increased. A long enough time to heat the soils to achieve good performance and economic results is approximately 8 hours.
- The moisture loss and change in structure of clay are the main factors controlling soil improvement as a result of increased shear strength and a more granular-type behaviour.
- Models based on artificial intelligence have successfully captured the non-linear relationships among variables, achieving high levels of accuracy (up to  $R^2=0.98$ ).

- The developed predictive equations provide reliable and practical tools for estimating the bearing capacity of thermally treated soft clay under different conditions.

#### 5. References

1. M. A. M. Al-Neami, "Reducing settlement of soft soils using local materials," *Engineering and Technology Journal*, vol. 28, no. 23 Part A, pp. 6649–6661, 2010.
2. S. Sasanian, *The behaviour of cement stabilised clay at high water contents*. The University of Western Ontario (Canada), 2011.
3. A. Ahmed, "Compressive strength and microstructure of soft clay soil stabilised with recycled bassanite," *Appl Clay Sci*, vol. 104, pp. 27–35, 2015.
4. A. Sukpunya and A. Jotisankasa, "Large simple shear testing of soft Bangkok clay stabilised with soil–cement-columns and its application," *Soils and Foundations*, vol. 56, no. 4, pp. 640–651, 2016.
5. B. Yuan *et al.*, "Addition of alkaline solutions and fibers for the reinforcement of kaolinite-containing granite residual soil," *Appl Clay Sci*, vol. 228, p. 106644, 2022.
6. B. Yuan *et al.*, "Sustainability of the polymer SH reinforced recycled granite residual soil: Properties, physicochemical mechanism, and applications," *J Soils Sediments*, vol. 23, no. 1, pp. 246–262, 2023.
7. Ö. Tan, L. Yılmaz, and A. S. Zaimoğlu, "Variation of some engineering properties of clays with heat treatment," *Mater Lett*, vol. 58, no. 7–8, pp. 1176–1179, 2004.
8. M. M. Abu-Zreig, N. M. Al-Akhras, and M. F. Attom, "Influence of heat treatment on the behavior of clayey soils," *Appl Clay Sci*, vol. 20, no. 3, pp. 129–135, 2001.

9. Q. Sun, W. Zhang, and H. Qian, "Effects of high temperature thermal treatment on the physical properties of clay," *Environ Earth Sci*, vol. 75, pp. 1–8, 2016.
10. J. Geng and Q. Sun, "Effects of high temperature treatment on physical-thermal properties of clay," *Thermochim Acta*, vol. 666, pp. 148–155, 2018.
11. Q. Hu *et al.*, "Microwave irradiation reinforcement of weak muddy intercalation in slope," *Appl Clay Sci*, vol. 183, p. 105324, 2019.
12. S. Zhang, Y. Ding, X. Lu, X. Mao, and M. Song, "Rapid and efficient disposal of radioactive contaminated soil using microwave sintering method," *Mater Lett*, vol. 175, pp. 165–168, 2016.
13. Z. Chen, H. Zhu, Z. Yan, L. Zhao, Y. Shen, and A. Misra, "Experimental study on physical properties of soft soil after high temperature exposure," *Eng Geol*, vol. 204, pp. 14–22, 2016.
14. Y. I. N. Tiefeng, L. I. U. Ganbin, and G. U. O. Zhen, "Theoretical and experimental study on thermal consolidation characteristics of typical soft clay in Ningbo region," *Building Structure*, vol. 44, no. 8, pp. 66–69, 2014.
15. Y. Chen, Z. Sun, Y. Cui, W. Ye, and Q. Liu, "Effect of cement solutions on the swelling pressure of compacted GMZ bentonite at different temperatures," *Constr Build Mater*, vol. 229, p. 116872, 2019.
16. J. J. Reinoso, B. García-Baños, J. M. Catalá-Civera, and J. F. Fernández, "A step ahead on efficient microwave heating for kaolinite," *Appl Clay Sci*, vol. 168, pp. 237–243, 2019.
17. H. Yao, J. Lu, H. Bian, and Z. Zhang, "Influence of microwave heating on the swelling properties of expansive soil in Hefei," *Case Studies in Thermal Engineering*, vol. 39, p. 102466, 2022.
18. A. Demirbas, "Fuel properties of hydrogen, liquefied petroleum gas (LPG), and compressed natural gas (CNG) for transportation," *Energy Sources*, vol. 24, no. 7, pp. 601–610, 2002.
19. F. Rahil, H. Baqir, and H. Alkabee, "Bearing capacity of soft clay improved by heating through different spacing cased boreholes," *Kufa Journal of Engineering*, vol. 10, no. 1, pp. 68–77, 2019.